

# A New Method for Lift-off of III-Nitride Semiconductors for Heterogeneous Integration

Ke Yan Zang · Davy W. C. Cheong ·  
Hong Fei Liu · Hong Liu · Jing Hua Teng ·  
Soo Jin Chua

Received: 19 March 2010 / Accepted: 1 April 2010 / Published online: 22 April 2010  
© The Author(s) 2010. This article is published with open access at Springerlink.com

**Abstract** The release and transfer of GaN epilayers to other substrates is of interest for a variety of applications, including heterogeneous integration of silicon logic devices, III-V power devices and optical devices. We have developed a simple wet chemical etching method to release high-quality epitaxial III-nitride films from their substrates. This method builds on a nanoepitaxial lateral overgrowth (NELO) process that provides III-Nitride films with low dislocation densities. NELO is accomplished using a nanoporous mask layer patterned on GaN substrates. Chemical removal of the SiO<sub>2</sub> layer after growth of III-Nitride overlayers causes fracture at the interface between the GaN film and the original GaN substrate, resulting in free-standing GaN films with nanostructured surfaces on one side. These layers can be transferred to other substrates, and the nano-structured surface can be used in photonic devices, or planarized for power devices.

**Keywords** Nanorod · Lift off · III-nitride semiconductor

Besides its applications in high efficiency and high power optoelectronics, e.g. Light Emitting Diodes (LEDs) and Laser Diodes (LDs), RF transistors, power electronics or photodetectors [1], III-nitride compound semiconductors nowadays attract high interests in utilizing their unique

optoelectronic properties, and integrating them heterogeneously with other material system to form more functional devices for future computational and telecommunication applications. A robust integration technique would allow the adding of high performance functionalities provided by GaN devices on other substrates for various advanced applications [2–6].

One approach to integrate III-nitride onto other material is direct heteroepitaxial growth on other substrates. For example, the growth of GaN structures on Si (100) or Si (110) substrates by molecular beam epitaxy (MBE), metalorganic chemical vapor deposition (MOCVD) have been reported [7, 8] for the integration of GaN devices with Si circuits. However, the material quality achieved through direct deposition is far from ideal. High density of deleterious threading dislocations in the active device layer due to large lattice mismatch and thermal mismatch inhibits the device performance. A more attractive approach is heterogeneous integration, where GaN structure that is independently grown and optimized, is released from its original substrate and transferred to favorable substrates. On-wafer integration of Si (100) MOSFETs and GaN HEMTs [9, 10], GaN optical interconnects [11] and thin film transistors on flexible substrate [2] have been demonstrated by using release and transfer techniques, such as laser lift off or chemical removal of substrates, layer transfer and wafer bonding technique.

To transfer the GaN devices, one of the key components involves releasing the GaN layers from its original substrate. The most cost effective approach to release GaN layers from its original substrate is to selectively etch a sacrificial layer. For example, Si released from Silicon on Insulator (SOI) and GaAs with AlAs as a sacrificial layers [12, 13]. The epitaxial lift off (ELO) method was well established since 1990s' due to the availability of the

K. Y. Zang (✉) · D. W. C. Cheong (✉)  
H. F. Liu · H. Liu · J. H. Teng · S. J. Chua  
Institute of Materials Research and Engineering,  
Agency for Science, Technology and Research (A\*STAR),  
3 Research Link, Singapore 117602, Singapore  
e-mail: ky-zang@imre.a-star.edu.sg

D. W. C. Cheong  
e-mail: davy-cheong@imre.a-star.edu.sg

etching selectivity between GaAs and AlAs. Many devices such as LEDs, lasers, MESFETs, and Photodiode were demonstrated based on the ELO method, [12–14] and heterogeneous integration was achieved in these system [15]. However, in the case of GaN material, the use of sacrificial layer etching is still far less optimized in view of the material quality achieved and the device performance [16–18]. Laser lift off (LLO) [19–23], Photoelectrochemical (PEC) lateral etching [24, 25], were alternative approaches to release GaN layers, however, these methods were costly and limits the scope of application. Therefore, there is a need for a low cost and effective chemical process to release GaN from its substrates without compromising the material quality.

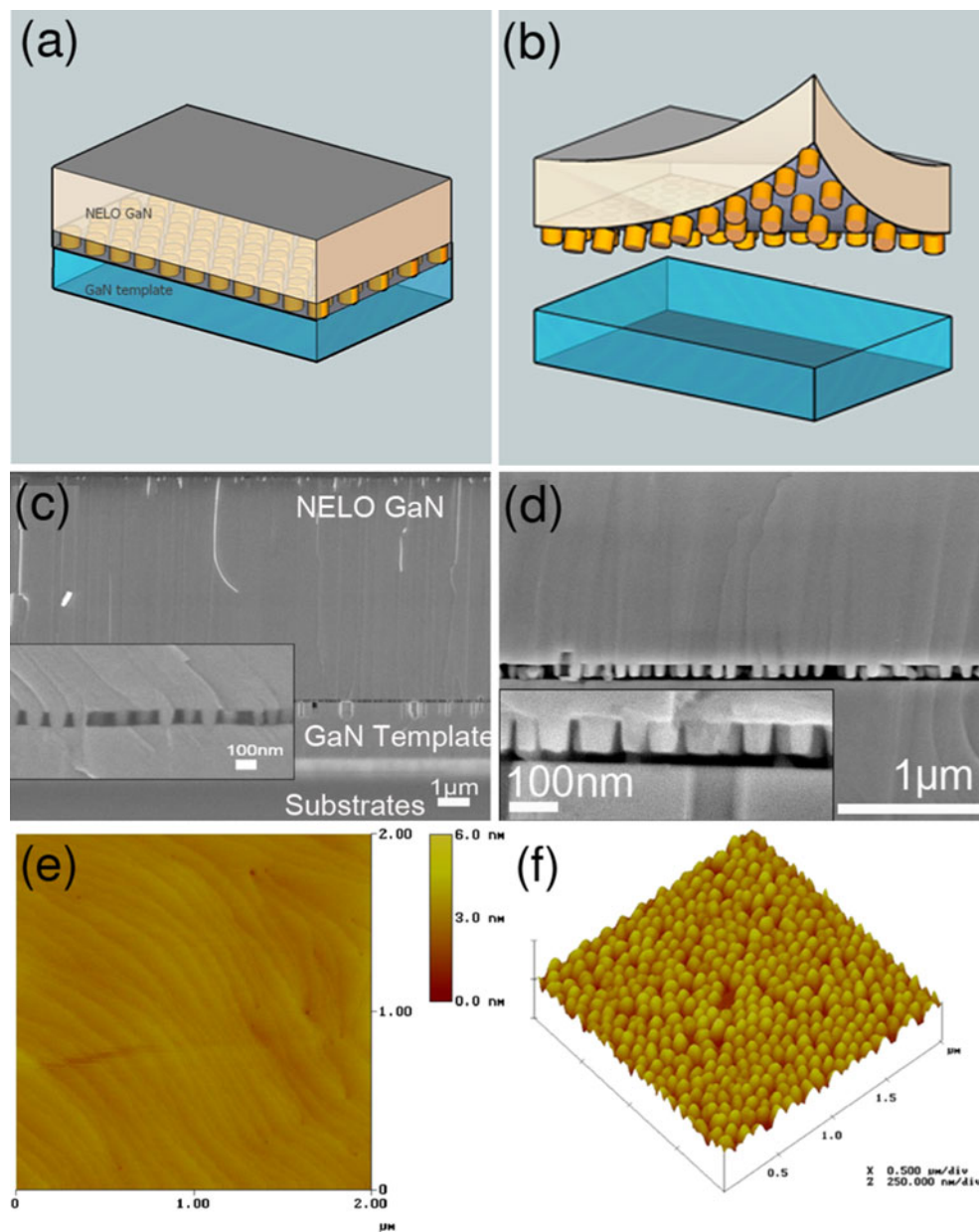
In this paper, we report a simple yet effective method to release high quality gallium nitride film from its substrate. The method utilizes nanoepitaxial lateral overgrowth (NELO) process, where GaN film is grown over nanoporous  $\text{SiO}_2$  mask layer. After chemical removal of the  $\text{SiO}_2$  nano-networks, the GaN with nanostructures releases spontaneously from the bottom GaN template layer, leading to a high quality GaN film with a nanostructured surface on one side. The key factors in this method are (1) nanostructured layer materials that can be selectively removed by wet chemicals. (2) the interaction between the nanostructured  $\text{SiO}_2$  layer and GaN nanostructures at the interface enabling the self release after chemical etching. This method offers the advantages of a low cost simple process with high etching selectivity and it produces GaN of good crystal quality. It could potentially lead to highly integrated and efficient III-V nanoelectronics, nanophotonics and power devices on silicon and mechanically flexible circuits.

Nano-Epitaxial Lateral Overgrown (NELO) GaN is grown over the nanostructured  $\text{SiO}_2$  mask on the GaN template. A GaN template layer  $\sim 1 \mu\text{m}$  was first grown on sapphire (0001) substrate using metalorganic chemical vapor deposition (MOCVD). A  $\sim 100 \text{ nm}$   $\text{SiO}_2$  film was then deposited on the GaN template layer using plasma enhanced chemical vapor deposition (PECVD), followed by fabricating anodized alumina (AAO) to create nanostructures. The detailed AAO anodization process was reported previously [26–28].  $\text{CF}_4$ -based inductively coupled plasma (ICP) etching was employed to transfer the nanopore structures of AAO into the  $\text{SiO}_2$  layer. The AAO template was then removed by chemical etchant, resulting in a closed packed nanopore arrays in the  $\text{SiO}_2$  layer on the surface of GaN. The mean pore diameter and interpore distance were of 60 and 110 nm, respectively. NELO GaN layer was then regrown on the GaN template covered with nanoporous  $\text{SiO}_2$  by using MOCVD. The detailed growth condition is reported previously elsewhere [26–28].

A typical GaN epitaxial layer structure is illustrated in Fig. 1a. The epitaxial film is simply undercut and released spontaneously from the GaN template upon the reaction of  $\text{SiO}_2$  with HF solution as shown in Fig. 1b. Figure 1c is a cross-sectional SEM image of NELO GaN layer grown on nanopatterned  $\text{SiO}_2$  mask on GaN template on sapphire substrates. Inset is a larger magnified image near the interface of the  $\text{SiO}_2$  mask. Bright contrast at the interface is the regrown GaN nanorods, and the dark contrast is the nanopatterned  $\text{SiO}_2$  mask. It was observed that the GaN nanostructures were grown inside the nanopores of  $\text{SiO}_2$ , bridging the top NELO GaN and the bottom GaN template. The diameter of the nanorods is  $\sim 60 \text{ nm}$  and the length is  $\sim 100 \text{ nm}$ , respectively. A direct observation of the separation of the NELO GaN from the GaN template is shown in Fig. 1d after exposing to HF solution. It is found from the image that the GaN nanorods separate from the GaN template while remaining attached to the top NELO GaN layer. To further study the surface morphology of the released layer, atomic force microscopy (AFM) images are taken on the flat top and nanostructured bottom surface. Figure 1e shows the AFM result of the top surface of the NELO GaN epilayer. It has been demonstrated by our previous study that NELO GaN shows improved crystal quality, better surface morphology and low defect density, which provides a better GaN material for high efficient optoelectronic devices. A light emitting diode (LED) fabricated from NELO GaN showed big improvement in the light output power [26–28]. Figure 1f shows the AFM images of the surface morphology of the nanostructures after spontaneously separating from the substrate. The dense nanorod arrays are clearly observed in the image. The diameter of the rod is  $\sim 60 \text{ nm}$ , and the height of the nanorod is  $\sim 100 \text{ nm}$ , which has the same dimension as the nanopores of  $\text{SiO}_2$ . This indicates that the separation starts at the interface of NELO GaN and the GaN template. The AFM findings are consistent with the SEM results.

Figure 2a, b shows cross-sectional transmission electron microscopy (TEM) image of a freestanding GaN with nanostructures after release from the substrates and a single nanorod. The released layer shows a very low defect density  $\sim 10^6 \text{ cm}^{-2}$ , compared to the common GaN on Si  $\sim 10^{10} \text{ cm}^{-2}$  or that on sapphire  $\sim 10^9 \text{ cm}^{-2}$ . No damage of GaN layer and GaN nanorods are observed. This indicates the high etching selectivity in this method. The nanostructures here play a dual role of making both the growth of high quality materials and the self release of NELO GaN possible. In addition, the nanostructures show uniform separation at the interface. Sharp, atomically flat surface can be seen at the GaN template after the mechanical release of the epitaxial layers. This indicates that the force responsible for the separation is uniformly distributed through the interface. The spontaneous self release

**Fig. 1** Schematic diagram of **a** structures of Nano epitaxial lateral overgrown (NELO) GaN. NELO GaN is grown by MOCVD through the nanopores of SiO<sub>2</sub> mask that are fabricated on GaN substrate. **b** Nanoepitaxial chemical release of NELO GaN epilayers by using HF solution. The chemical removal of SiO<sub>2</sub> mask leads to the NELO GaN together with GaN nanorods separate from the GaN template. **c** Cross sectional SEM images of NELO GaN before release and **d** after release; *Insets* are enlarged images near the interface of nanostructured SiO<sub>2</sub> mask and GaN nanorods. **e** AFM images of *top* surface of released NELO GaN epilayer showing low defect density **f** 2D view of *bottom* surface of released NELO GaN showing the dense nanorod arrays. The diameter of the rod is ~60 nm, and the height of the nanorod is ~100 nm. It indicates that the separation happens at the interface of NELO GaN and the GaN template



mechanism is studied using Molecular Dynamics (MD) simulation. Figure 2c shows the photoluminescence spectra (PL) measured from the top and bottom surface after release. The nanostructured surface shows a stronger PL emission compared to the flat top surface. This indicates that the nanostructures enhance the light extraction efficiency. To increase the light extraction efficiency in GaN based optoelectronic devices, patterned substrate [29–32], roughening and patterning the GaN surface with photonic crystal structures [33–35] were used. Hence, this process is therefore a simple and low cost method to produce LED devices with better performance.

Molecular dynamics (MD) simulations were carried out to understand the separation mechanism responsible for the

spontaneous lift off of GaN films observed in the experiments. The functional form of a two-body interatomic potential used in the model is as follows [36]:-

$$u_{ij} = \frac{Z_i Z_j e^2}{4\pi\epsilon_0 r_{ij}} + f_0(b_i + b_j) \exp\left(\frac{a_i + a_j - r_{ij}}{b_i + b_j}\right) + D_{1ij} \exp(-\beta_{1ij} r_{ij}) + D_{2ij} \exp(-\beta_{2ij} r_{ij}) - \frac{c_i c_j}{r_{ij}^6}$$

Coulombic interaction is expressed in the first term of interatomic potential; the second term is the Gilbert-type short-range repulsion, while covalent bonding and repulsion of the modified Morse types is represented by the third and fourth terms respectively. The last term represents Van der Waals interactions.  $r_{ij}$  is the distance

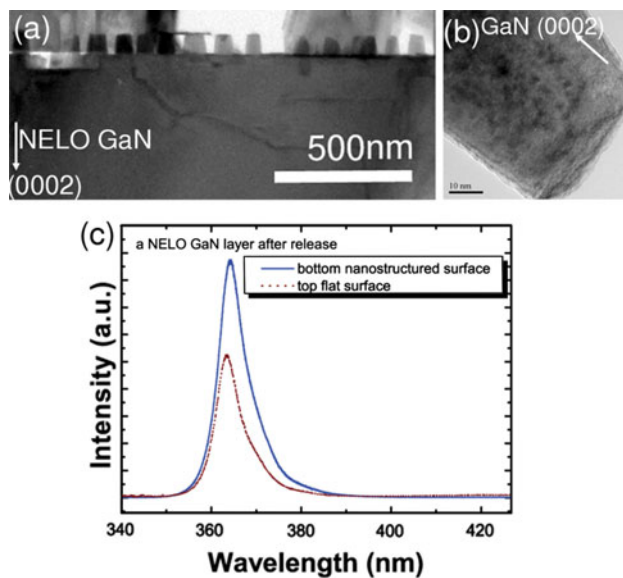


**Fig. 2** Cross-sectional transmission electron microscopy images of **a** NELO GaN after lift off from the GaN template, **b** a nanorod after lift-off. Micro-photoluminescence of **c** NELO GaN flat surface and the surface with nanorods after release from substrates

between the  $i$ th and  $j$ th atoms,  $Z_i$  is the effective charge for each atom,  $\epsilon_0$  is the dielectric constant of the vacuum,  $f_0$  is the constant for unit conversion [41.86 kJ/(nm mol)],  $a_i$  is the repulsion radius,  $b_j$  is the softness parameter,  $D_1$ ,  $D_2$ ,  $\beta_1$  and  $\beta_2$  are covalent coefficients, and  $c_i$  and  $c_j$  are the Van der Waals coefficient. Detailed descriptions of the parameters are obtained in Ref. 24. The time evolution trajectory of the atoms is solved using Verlet algorithm. The time step of 2 fs is used in the present study. All atomic pairs between Ga and N are taken into account and calculated for all the potentials in the equation.

A single GaN nanorod between the  $\text{SiO}_2$  mask with periodic boundary in the plane of the film is considered in our simulation model (shown in Fig. 3a). The effective lattice spacing of GaN atoms at the base were determined from the Raman shift of the GaN template, while the top surface of the model is chosen as a free surface where the atoms at the surface is nearly mechanically unconstrained [37–41] and built-in stress which is responsible for the spontaneous lift off of the GaN film is incorporated in the model. The built-in stress is suggested to originate from the

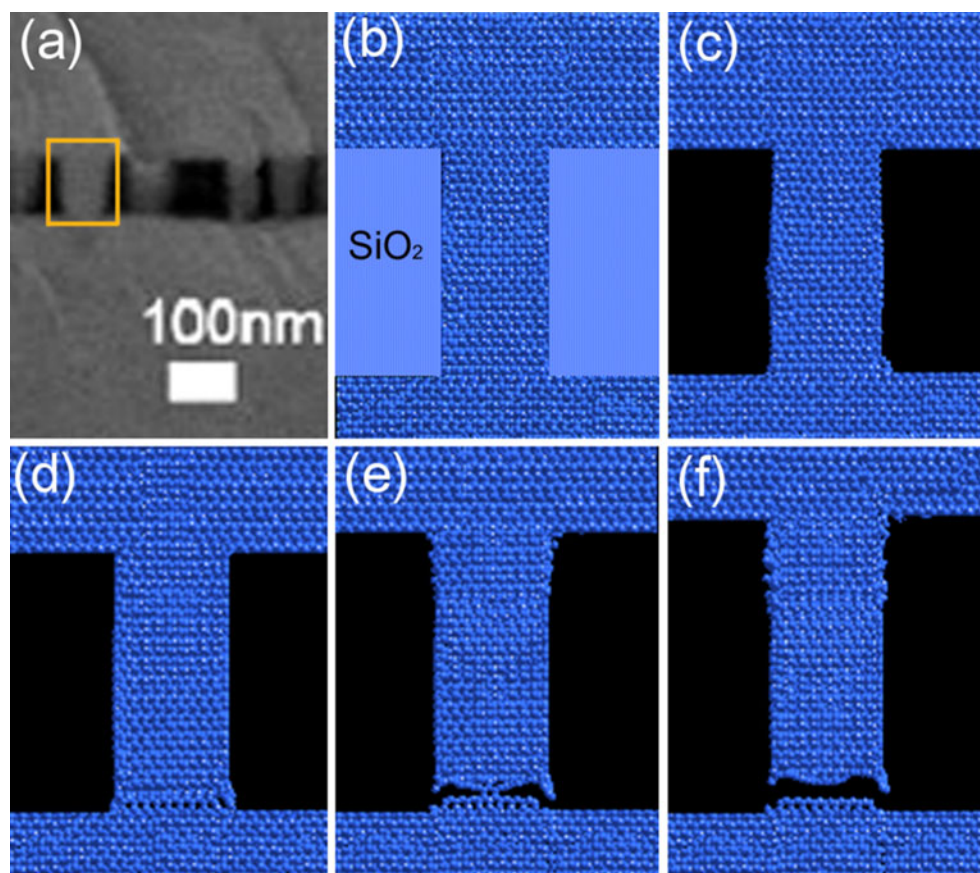


**Fig. 3** Molecular Dynamic simulation results of the separation of NELO GaN nanostructures from GaN template near the  $\text{SiO}_2$  mask. **a** Cross-sectional SEM image of NELO GaN near the nanostructured  $\text{SiO}_2$  mask; the square illustrates the unit that was chosen in the MD simulation; **b–f** are the MD simulation results at time of 0, 60, 100,

140 and 180 ps after chemical removal of  $\text{SiO}_2$ , respectively. The results indicate that there is a large strain field at the corners of the GaN nanorods, and the built-in stress caused by the interaction between GaN and  $\text{SiO}_2$  mask contributed to the fracture at the interface between the GaN film and the original GaN substrate

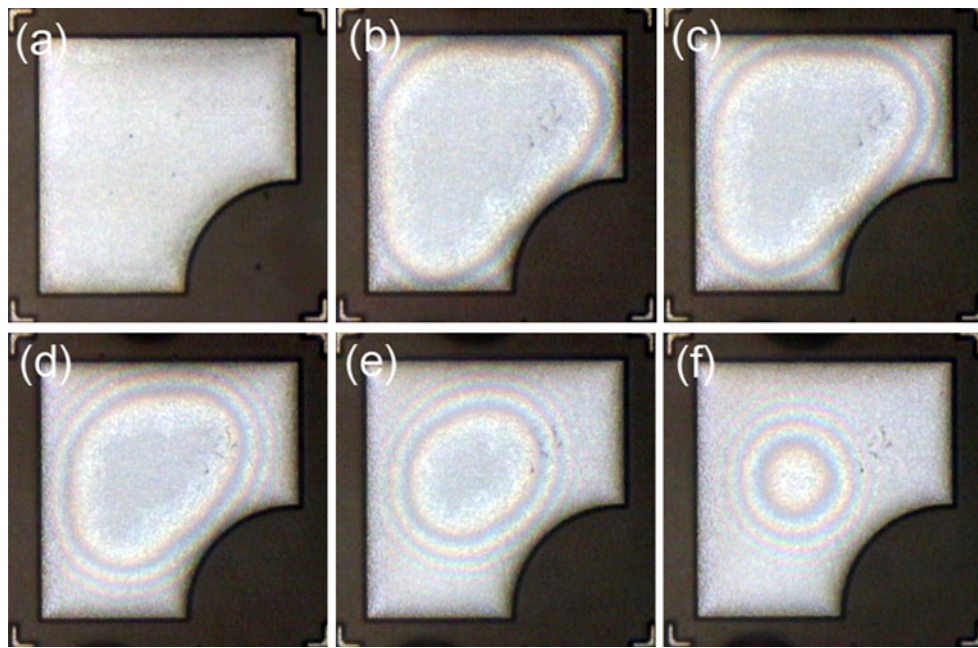


**Fig. 4** Microscopic images of the HF undercutting of a  $300 \times 300 \mu\text{m}$  GaN mesa with etching time of **a** 3 min, **b** 6 min, **c** 9 min, **d** 12 min, **e** 15 min, and **f** 18 min, respectively

interaction between the GaN and the  $\text{SiO}_2$  mask as reported by Ztykiewicz et al. [37–41]. The interaction between GaN and  $\text{SiO}_2$  contributes a large strain field near the mask region in the micro scale epitaxial lateral overgrown GaN system and causes the relaxation of the film after removal of the  $\text{SiO}_2$  mask. A large strain field near the mask is also reported by Liu et al. by using continuum elasticity theory on stress analysis of selective epitaxial growth of GaN [42]. The simulation result shows that there is no yielding in the GaN film when the GaN is initially bonded to the  $\text{SiO}_2$  mask (shown in Fig. 3b). Once the  $\text{SiO}_2$  mask is removed, it is evident from the simulation result in Fig. 3c that a large lattice distortion is observed at the corners of the GaN nanorod, and the GaN nanorod starts to yield and eventually crack at the bottom of the nanorods (Fig. 3d–f). This simulation result is consistent with the experimental observations and showed that the stresses caused by the interaction between the GaN and the mask are the main driving force for the spontaneous release of NELO GaN. It also shows that the stress field generated by the GaN and  $\text{SiO}_2$  interaction results in the NELO GaN separating from the GaN template on the template side. The numerical simulation therefore provided a qualitative understanding of the mechanisms involved in the spontaneous release of NELO GaN from the template.

To understand the etching behavior,  $300 \times 300 \mu\text{m}^2$  mesas are created by photolithography patterning and inductive coupled plasma dry etching (ICP) to etch through the  $\text{SiO}_2$  mask layer. The GaN layer was then undercut in a 26.5% diluted HF acid at room temperature without

agitation. By using in situ optical microscopy, optical fringes and a bright contrast between the undercutting region and non-undercutting region were observed (shown in Fig. 4a–f). It is observed that the etching starts at the edge of the sample, where the HF reacts with the  $\text{SiO}_2$ . The etching continues towards the center of the sample until the complete separation of the film. The lateral etch rate is estimated at  $\sim 15 \mu\text{m}/\text{min}$ . After the etching is completed, the NELO GaN mesa was observed to remain at its original position, held by a weak attractive force. Polydimethylsiloxane (PDMS) can be used to contact the released GaN for transferring to other substrates. An alternative approach to transfer the GaN layer is to bond the GaN surface to more favorable substrates before releasing in HF solution. We believe that, if combined with an improved transfer and bonding technology, this lift-off method could provide a simple and yet effective way to integrate GaN-based devices with Si circuits or other favorable substrates for power devices and high efficiency optoelectronic devices.

In conclusion, a simple and reliable method to form high quality freestanding GaN film is demonstrated. The GaN thin film is grown through a  $\text{SiO}_2$  template with nano-openings on top of a GaN layer and released later by HF based wet chemical etching. The self-release of the GaN thin film is enabled by the built-in stress originating from the interaction of GaN and the  $\text{SiO}_2$  mask. The GaN film produced by this method offers better crystal quality, beneficial to high efficiency and high power applications. In addition, the nanostructures in GaN produced by this method can lead to improved light extraction for LED

applications and can be used to create hierarchical structures for nanophotonic applications. The method is potentially useful for applications that involve heterogeneous integration of III-nitride based optical and power devices on Si or flexible substrates, as well as various other applications, e.g. MEMs system, microcavities and microoptics systems and nanophotonics.

**Acknowledgments** This project was funded by Agency for Science, Technology and Research (A\*STAR) of Singapore under grant No. IMRE/09-1P0605.

**Open Access** This article is distributed under the terms of the Creative Commons Attribution Noncommercial License which permits any noncommercial use, distribution, and reproduction in any medium, provided the original author(s) and source are credited.

## References

1. S. Nakamura, S. Pearton, G. Fasol, *The Blue Laser Diode* (Springer, Berlin, 2000)
2. J.-H. Ahn, H.-S. Kim, K.J. Lee, S. Jeon, S.J. Kang, Y. Sun, R.G. Nuzzo, J.A. Rogers, *Science* **314**, 1754 (2006)
3. J.A. Chediak, Z. Luo, J. Seo, N. Cheung, L.P. Lee, T.D. Sands, *Sens. Actuators A Phys.* **111**, 1 (2004)
4. Y. Dong, B. Tian, T.J. Kempa, C.M. Lieber, *Nano Lett.* **9**, 2183 (2009)
5. K. Aoki, D. Guimard, M. Nishioka, M. Nomura, S. Iwamoto, Y. Arakawa, *Nat. Photonics* **2**, 688 (2008)
6. H. Matsubara, S. Yoshimoto, H. Saito, J. Yue, Y. Tanaka, S. Noda, *Science* **319**, 445 (2008)
7. S. Joblot, F. Semond, Y. Cordier, P. Lorenzini, J. Massies, *Appl. Phys. Lett.* **87**, 133505 (2005)
8. F. Schulze, O. Kisel, A. Dadgar, A. Krtschil, J. Blasing, M. Kunze, I. Daumiller, T. Hempel, A. Diez, R. Clos, A. Krost, *J. Cryst. Growth* **299**, 399 (2007)
9. J.W. Chung, J.K. Lee, E.L. Piner, *IEEE Electron Device Lett.* **30**, 1015 (2009)
10. N.M. Jokerst, M.A. Brooke, S.-Y. Cho, S. Wilkinson, M. Vrazel, S. Fiike, J. Tabler, Y.J. Joo, S.-W. Seo, D.S. Wills, A. Brown, *IEEE J. Sel. Top. Quantum Electron.* **9**, 350 (2007)
11. N.W. Cheung, *Proceedings of 7<sup>th</sup> International Conference on solid-state and integrated circuits technology*, **1–3**, 2167 (2004)
12. E. Yablonovitch, E. Kapon, T.J. Gmitter, C.P. Yun, R. Bhat, *IEEE Photonics Technol. Lett.* **1**, 41 (1989)
13. H. Park, S. Kim, S. Kwon, Y. Ju, J. Yang, J. Baek, S. Kim, Y. Lee, *Science* **305**, 1444 (2004)
14. I. Pollentier, P. Demeester, A. Ackaert, L. Buydens, P.V. Daele, R. Baets, *Electron. Lett.* **26**, 193 (1990)
15. E. Yablonovitch, in *Properties of Gallium Arsenide*, 3rd edn. ed. by MIR Brozel, G.E. Stillman (INSPEC, the Institute of Electrical Engineering, London, 1996), pp. 672–676
16. S.W. Lee, J.S. Ha, Hyun.-Jae. Lee, Hyo.-Jong. Lee, H. Goto, T. Hanada, T. Goto, K. Fujii, M.W. Cho, T. Yao, *Appl. Phys. Lett.* **94**, 082105 (2009)
17. D.J. Rogers, F.H. Teherani, A. Ougazzaden, S. Gaultier, L. Divay, A. Lusson, O. Durand, F. Wyczisk, G. Garry, T. Monteiro, M.R. Correira, M. Peres, A. Neves, D. McGrouther, J.N. Chapman, M. Razeghi, *Appl. Phys. Lett.* **91**, 071120 (2007)
18. K.J. Lee, M.A. Meitl, J.H. Ahn, J.A. Rogers, R.G. Nuzzo, V. Kumar, I. Adesida, *J. Appl. Phys.* **100**, 124507 (2006)
19. W.S. Wong, T. Sands, *Appl. Phys. Lett.* **77**, 2822 (2000)
20. W.S. Wong, T. Sands, N.W. Cheung, M. Kneissi, D.P. Bour, P. Mei, T. Romano, N.M. Johnson, *Appl. Phys. Lett.* **75**, 1360 (1999)
21. M.K. Kelly, R.P. Vaudo, V. Phanse, L. Gorgens, O. Ambacher, M. Stutzmann, *Jpn. J. Appl. Phys.* **38**, L217 (1999)
22. C.R. Miskys, M.K. Kelly, O. Ambacher, M. Stutzmann, *Phys. Stat. Sol. (c)* **0(6)**, 1627 (1999)
23. A. Khan, K. Balakrishnan, T. Katona, *Nat. Photonics* **2**, 77 (2008)
24. M.S. Minsky, M. White, E.L. Hu, *Appl. Phys. Lett.* **68**, 1531 (1996)
25. Y.S. Choi, K. Hennessy, R. Sharma, E. Haberer, Y. Gao, S.P. DenBaars, S. Nakamura, E.L. Hu, *Appl. Phys. Lett.* **87**, 243101 (2005)
26. Y.D. Wang, K.Y. Zang, S.J. Chua, M.S. Sander, S. Tripathy, C.G. Fonstad, *J. Phys. Chem. B* **110**, 11081 (2006)
27. Y.D. Wang, K.Y. Zang, S.J. Chua, S. Tripathy, H.L. Zhou, C.G. Fonstad, *Appl. Phys. Lett.* **88**, 211908 (2006)
28. K.Y. Zang, S.J. Chua, J.H. Teng, N.S. Ang, A.M. Yong, S.Y. Chow, *Appl. Phys. Lett.* **92**, 243126 (2008)
29. A. Bell, R. Liu, F.A. Ponce, H. Amano, I. Akasaki, D. Cherns, *Appl. Phys. Lett.* **82**, 349 (2003)
30. K. Tadatomo, H. Okagawa, Y. Ohuchi, T. Tsunekawa, Y. Imada, M. Kato, T. Taguchi, *Jpn. J. Appl. Phys.* **40**, L583 (2001)
31. I. Schnitzer, E. Yablonovitch, C. Caneau, T.J. Gmitter and A. Scherer *A* **19**, *Appl. Phys. Lett.* **63**, 2174 (1993)
32. M. Yamada, T. Mitani, Y. Narukawa, S. Shioji, I. Niki, S. Sonobe, K. Deguchi, M. Sano, T. Mukai, *Jpn. J. Appl. Phys.* **41**, L1431 (2002)
33. R.C. Tu, C.C. Chuo, S.M. Pan, Y.M. Fan, C.E. Tsai, T.C. Wang, C.J. Tun, G.C. Chi, B.C. Lee, C.P. Lee, *Appl. Phys. Lett.* **83**, 3608 (2003)
34. T.N. Oder, K.H. Kim, J.Y. Lin, H.X. Jiang, *Appl. Phys. Lett.* **84**, 466 (2004)
35. C.F. Lin, J.H. Zheng, Z.J. Yang, J.J. Dai, D.Y. Lin, C.Y. Chang, Z.X. Lai, C.S. Hong, *Appl. Phys. Lett.* **88**, 083121 (2006)
36. K. Harafuji, T. Tsuchiya, K. Kawamura, *J. Appl. Phys.* **96**, 2501 (2004)
37. Z.R. Zytkiewicz, *Proc. SPIE* **4413**, 112 (2001)
38. P. Fini, A. Munkholm, C. Thompson, G.B. Stephenson, J.A. Eastman, M.V.R. Murty, O. Auciello, L. Zhao, S.P. DenBaars, J.S. Speck, *Appl. Phys. Lett.* **76**, 3893 (2000)
39. J.M. Wagner, F. Bechstedt, *Phys. Rev. B* **66**, 115202 (2002)
40. J.W. Chen, Y.F. Chen, H. Lu, W.J. Schaff, *Appl. Phys. Lett.* **87**, 041907 (2005)
41. S.C. Jain, A.H. Harker, A. Atkinson, K. Pinardi, *J. Appl. Phys.* **78**, 1630 (1995)
42. Q.K.K. Liu, A. Hoffmann, H. Siegle, A. Kaschner, C. Thomsen, J. Christen, F. Bertram, *Appl. Phys. Lett.* **74**, 3122 (1999)